Asian Journal of Chemistry; Vol. 34, No. 3 (2022), 685-694

ASIAN JOURNAL OF CHEMISTRY

https://doi.org/10.14233/ajchem.2022.23301

Antimicrobial, Cytotoxicity and Molecular Docking Study of New Quinoline Schiff Base and its Metal(II) Complexes

B.T. VIBHUTE[1,*], B.D. AGHAV[1], B.P. MORE[2], R.O. BELLAMKONDA[3] and S.K. PATIL[1]

[1]Department of Chemistry, Changu Kana Thakur Arts, Commerce and Science College, New Panvel-Raigad, Navi Mumbai-410206, India
[2]Department of Chemistry, M.V.P. Samaj's Arts, Commerce and Science College, Nandgaon-423106, India
[3]Department of Chemistry, Sreyas Institute of Engineering and Technology, Bandlaguda, Nagole-500068, India

*Corresponding author: E-mail: vbtchem@gmail.com

Received: 13 May 2021; *Accepted*: 24 December 2021; *Published online*: 14 February 2022; AJC-20704

A new quinoline Schiff base ligand was synthesized by the reaction of 2-hydroxy-7-methylquinolin-3-carbaldehyde and 4-methylbenzene sulfonohydrazide. Synthesized Schiff base further utilized for the formation of stable metal complexes with Cu(II), Ni(II), Co(II) and Cd(II) metal salts and characterized by different spectroscopic techniques *i.e.* ^{1}H NMR, ^{13}C NMR, FT-IR, UV-visible, ESR, MASS and TGA. The low molar conductance values indicate that synthesized metal(II) complexes were non-electrolytes. The magnetic moment value indicates that Cu(II), Ni(II) and Co(II) complexes were paramagnetic. Further, these compounds were screened for inhibition activity against four bacterial strains, three fungal strains and cytotoxicity against the A-549 and MCF-7 cell lines by using the MTT method. Among the synthesized complexes, metal complexes exhibited excellent anticancer activity against the human lung cancer cell line (A-549). Schiff base and its Cd(II) complex showed good antibacterial activity. Furthermore, molecular docking study shows the significant binding affinity of metal complexes with tubulin protein. Present study proposed that all the synthesized Schiff base metal(II) complexes have excellent biological activity and could be act as potential anticancer agents.

Keywords: Schiff base, Sulfonohydrazide, Quinoline, MIC, Cytotoxicity.

INTRODUCTION

Schiff bases are an interesting class of compounds, which attracts considerable attention of researchers. This is because of their diversity in its property, structural variability and their easy preparation [1,2]. They play an important role in the formation of the chelate compounds [3]. Schiff base having electrons reaches functional groups such as -OH, -SH and $-NH_2$ at adjacent positions to the azomethine group help to develop coordination with metal ions, which form stable complexes [4-12].

Metal complexes derived from Schiff bases are an interesting area of research. Such complexes have been widely used in biological [13-20], analytical [21,22] and catalyst [23-25] field. Form the study, it was observed that the coordination of Schiff base with metal ions increase the biological activity of Schiff base [26,27].

Among the heterocyclic compounds, quinoline and its derivatives were found to be a significant class in the biological field [28]. Several derivatives of quinoline are found to be effective antibacterial [17], antimicrobial [29], fungicides [17], antiviral [30], anti-inflammatory [31,32] and antitumor activities [33]. Simultaneously, metal complexes derived from quinoline Schiff bases have extensive applications in different areas such as, catalyst in various types of reactions [34,35], dyes in solar cells [36], corrosion inhibitor [37], antioxidant [2], cytotoxic [28], DNA cleavage [38], anticancer [39], *etc*.

To find better antimicrobial and anticancer drug, we have designed and synthesized novel quinoline Schiff base and its metal(II) complexes. Synthesized compounds were confirmed by different analytical techniques and studied for its anti-bacterial, antifungal and cytotoxicity activities.

EXPERIMENTAL

All the required chemicals were purchased from Sigma-Aldrich Chemical Co., (USA), Molychem Chemical Supplier (Mumbai, India) and used as such for further synthesis. Fourier

transform infrared spectroscopy (FTIR) spectra were recorded on a Nicolet iS10, thermos Scientific, USA spectrophotometer using KBr pellets in the range of 4000-400 cm^{-1}. Proton nuclear magnetic resonance (^1H and ^{13}C NMR) spectra of Schiff base were measured in DMSO-d_6 solvent on a Bruker Avance 400 MHz and 100MHz spectrometers, respectively. Electronic (UV-Visible) spectra were recorded using Carry 100 UV-visible spectrophotometer. Electron spins resonance (ESR) spectra of Cu(II) complex were performed on the JES-FA200 ESR Spectrometer. Thermogravimetric analysis (TGA) of metal complexes was performed on Mettler-Toledo instrument at the heating rate of 20 ºC/min with a temperature range of 25 to 1000 ºC. Electrospray ionization mass spectra (ESIMS) were recorded on a Waters Micromass Q-T of Micro with atmospheric pressure chemical ionization (APCI) sources. Elemental analyses were performed on a FLASH EA 1112 series instrument. The magnetic moments were measured by the Gouy method at 25 ºC using the MKl Johnson Matthey model. Molar conductance was measured on DDS-11C type conductivity Bridge in DMSO solution at a concentration of 10^{-3} M.

Synthesis of quinoline Schiff base ligand (HL): 2-Chloro-7-methylquinoline-3-carbaldehyde was synthesized using Vilsmeier-Haack reaction as reported method [40]. The synthesized 2-chloro-7-methylquinoline-3-carbaldeyde was further used for the formation of 2-hydroxy-7-methylquinoline-3-carbal-deyde. 2-Chloro-7-methylquinoline-3-carbaldeyde (20 mmol) and 2 mL H_2O was dissolved in 4 mL acetic acid and refluxed for 4 h. The progress of the reaction was checked by TLC. The obtained product, 2-hydroxy-7-methylquinoline-3-carbaldeyde was washed with distilled water and recrystallized in absolute ethanol. The recrystallized 2-hydroxy-7-methyl-quinoline-3-carbaldeyde was further used for the synthesis of the final Schiff base ligand. For the formation of the final ligand, a mixture of 2-hydroxy-7-methylquinoline-3-carbaldeyde (1 mmol), 4-methylbenzenesulfonohydrazide (1 mmol) and 5-10 drops acetic acid in 15 mL ethanol was placed in a round bottom flask. The mixture was refluxed at 75 ºC for 4 h. The progress of the reaction was checked by TLC. The reaction mixture was quenched with crushed ice and extracted with ethyl acetate. The organic extracts were washed with brine solution and dried over anhydrous sodium sulphate. The solvent was evaporated under reduced pressure to obtain the corresponding crude compound, which was purified with ethanol (**Scheme-I**). ^1H NMR: (100 MHz, DMSO-d_6, δ ppm): 11.57 (s, 1H, NH),

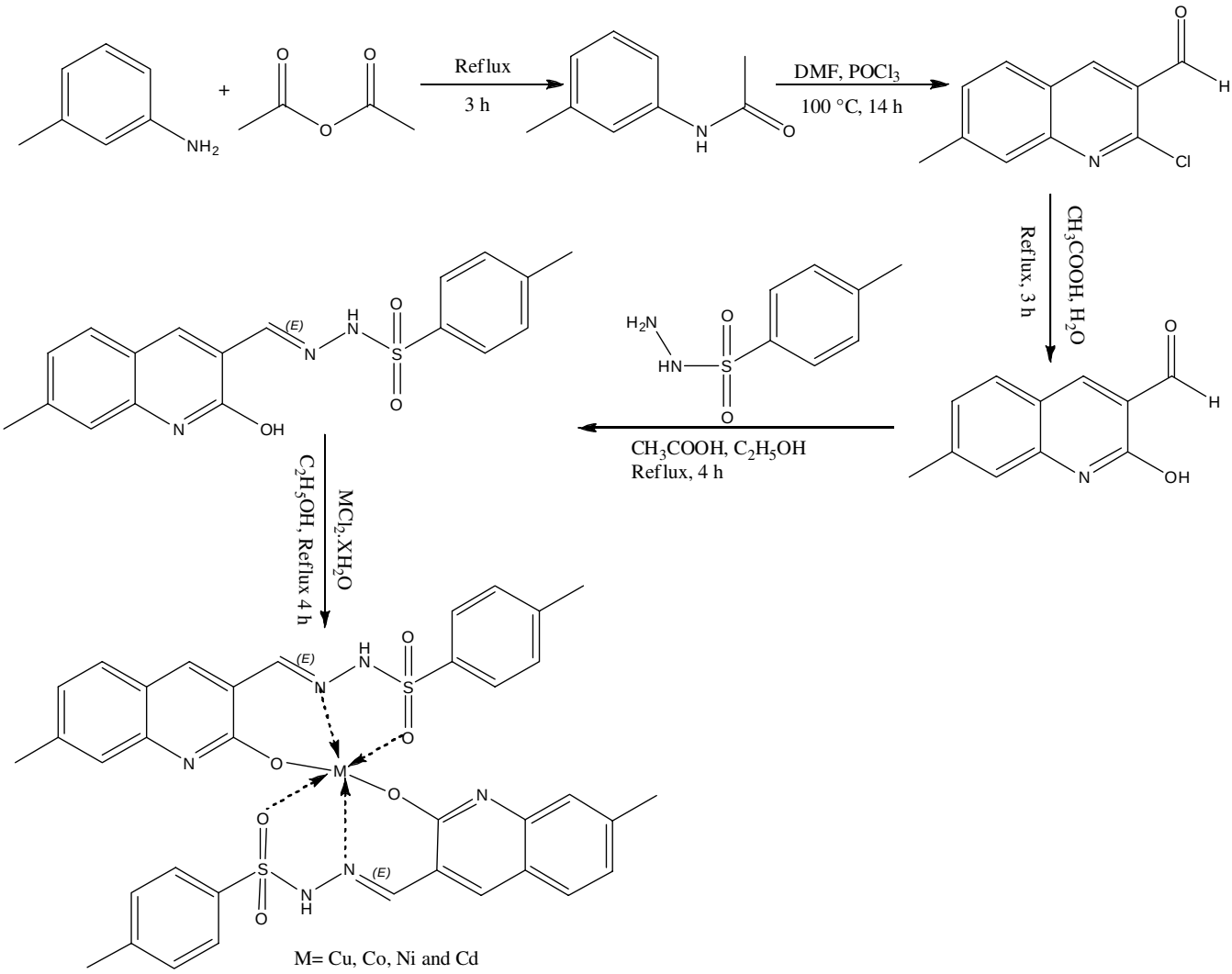

Scheme-I: Synthesis of Schiff base and its metal complexes

11.18 (s, 1H, OH), 8.12 (s, 1H, Ar-H), 8.07 (s, 1H, Ar-H), 7.73-7.71 (d, 2H, Ar-H, *J* = 7.5 Hz), 6.89-6.87(d, 2H, Ar-H, *J* = 7.5 Hz) 7.56 (s, 1H, Ar-C=CH), 7.38-7.36 (d, 1H, Ar-H, *J* = 8 Hz), 7.22-7.20 (d, 1H, Ar-H, *J* = 8 Hz) and 2.30 (s, 6H, -CH_3); ^{13}C NMR (100 MHz, DMSO-d_6, δ ppm): 161.84, 143.48, 142.43, 141.93, 139.29, 136.45, 135.19, 129.45, 128.45, 127.45, 124.18, 123.90, 117.21, 115.43, 21.90 and 21.51.

Synthesis of metal(II) complexes: A hot ethanolic solutions of metal(II) chloride (5 mL , 0.0015 mol) were added to 30 mL hot ethanolic ligand solution (0.0030 mol) in 250 mL round bottom flask. The reaction mixture was stirred for 30 min and few drops of 5% NaOH solution were added to maintain basic condition of the reaction. Further, the reaction mixture was refluxed for 4 h to complete the formation of the metal(II) complexes. The formed coloured metal(II) complexes were washed with distilled water followed by ethanol.

Biological study

Antibacterial study: The broth dilution method was used to measure the minimum inhibitory concentration (MIC) of prepared compounds [41]. Dimethyl sulfoxide (DMSO) was used as a solvent for diluent and it has no biological effect on selected bacterial strain [42]. In this study, two Gram-negative bacteria *viz.*, *Escherichia coli* (MTCC 443) and *Pseudomonas aeuruginosa* (MTCC 1688) and two Gram-positive bacteria *viz.*, *Staphylococcus aureus* (MTCC 96) and *Staphylococcus pyogenus* (MTCC 442) were tested against the synthesized Schiff base ligand and its metal(II) complexes. Chloramphenicol and ampicillin were used as the standard drugs for reference. Serial dilutions of Schiff base ligand and its metal (II) complexes were prepared for the primary and secondary screening. The control plate with no prepared compounds and drug was subculture spreading evenly over a plate suitable for the growth of selected bacterial pathogens and kept overnight at 37 ºC in incubator. The MIC of the control bacterial strain was assessed to check the efficacy of the reference drug concentrations. The lowest concentration was recorded as the MIC. The amount of growth from the control plate before incubation was compared. Synthesized compounds were diluted to 2000 µg/mL concentration as a stock solution. In primary screening, 125, 250 and 500 µg/mL concentrations of synthesized compounds were taken. The synthesized compounds found active in primary screening were further tested in the second set of dilutions against all the selected pathogens. The particles found active in primary screening were diluted similarly to 100, 50, 25, 12.5, 6.250, 3.125 and 1.5625 µg/mL concentrations. The MIC was considered for the dilution showing at least 99% inhibition.

Antifungal study: The antifungal activity of the synthesized compounds was studied with three fungal strains *viz.*, *Aspergillus clavatus* (MTCC 1323), *Candida albicans* (MTCC 227) and *Aspergillus niger* (MTCC 282) using agar dilution protocol [41]. To determine MIC, a stock solution of synthesized compounds was prepared in DMSO and then incorporated in a specified quantity of sterile molten dextrose agar for antifungal screening. The inoculate was prepared by taking a stock to about 100 mL of nutrient broth in 250 mL sterilized and clean conical flasks. The conical flasks were incubated at 27 ºC for 24 h before the experiment. The plates were kept under aseptic conditions to allow the diffusion of the solution properly into potato-dextrose agar medium. Then, the plates were incubated at 25 ºC for 48 h. The highest dilution displaying at least 99% inhibition zone was taken as MIC with nystatin and graseofulvin as a standard reference drugs. The triplicate analysis was performed to minimize errors.

Cytotoxicity: The cells were seeded at a density of approximately 5×10^3 cells well in a 96-well flat bottom microtitre plate and maintained at 37 ºC overnight in 95% humidity and 5% CO_2. Different concentrations (50, 40, 30, 20, 10, 5 µM) of samples were treated and the cells were incubated for the next 48 h. The cells in well were washed twice with phosphate buffer saline (PBS) and 20 µL of MTT [3-(4,5-dimethythiazol-2-yl)-2,5 diphenyltetrazolium bromide] staining solution (5 mg mL^{-1} in phosphate buffer saline) was added to each well and the plate was incubated at 37 ºC. After 4 h, 100 µL DMSO was added to each well to dissolve the formant crystals and the absorbance was recorded at 570 nm using a microplate reader.

Molecular docking study: To investigate the binding mode of various drug-metal complexes (Cd, Co, Cu and Ni) with β-tubulin receptor, molecular docking was performed using Auto Dock software [43]. The microtubules are essential in cell division [44]. The inhibition of microtubules structure leads to disturb its dynamics that's leads to cell apoptosis and death [45]. Hence, we used β-tubulin as target receptor for the molecular docking study, to understand the binding mode of various metal-drug complexes with β-tubulin. The crystal structure of tubulin (1JFF.pdb) was retrieved from the protein database. The three dimensional atomic coordinates of the metal complexes (Cd, Co, Cu and Ni) were built Discovery Studio Visualizer [46]. The grid box of 80 × 80 × 80 was built around the paclitaxel binding pocket with grid spacing 0.375Å. Herein, we performed a local docking protocol, to explore the binding mode of metal-drug complexes using AutoDock. Here, Lamarckian Genetic Algorithm was used for molecular docking and output conformations were further clustered using an all-atom RMSD with a cut-off of 4 Å. The lowest binding energy conformation were further utilized for bonding and non-bonding interactions analysis and visualization using (DeLano, 2002) and Discovery Studio visualizer [46] and PyMol [47], respectively.

RESULTS AND DISCUSSION

From the elemental analysis data (Table-1), it was confirmed that the synthesized Schiff base ligand and its metal(II) complexes are completely formed. All the prepared compounds were subjected to molar conductance in DMSO solvent at the concentration of 10^{-3} M. The molar conductance of the metal complexes was found to be in the range of 47-68 Ω^{-1} cm^2 mol^{-1}. From the obtained values (Table-1), it was proved that all the synthesized metal(II) complexes were non-electrolyte with evidence for the absence of water molecules in the coordination sphere.

TABLE-1
PHYSICAL AND ANALYTICAL DATA OF QUINOLINE SCHIFF BASE LIGAND AND ITS METAL(II) COMPLEXES

Compounds	Yield (%)	m.p. (°C)	Λ_m (cm^2 Ω^{-1} mol^{-1})	μ_{eff} (B.M.)	m.w.	Elemental analysis (%): Found (calcd.)			
						C	N	H	S
$C_{18}H_{17}N_3O_3S$	81	220-222	–	–	355.10	59.98 (60.83)	11.52 (11.82)	4.56 (4.82)	8.65 (9.02)
$[(C_{18}H_{17}N_3O_3S)_2Cu]$	73	>300	58	1.78	772.35	55.85 (55.98)	10.86 (10.88)	4.14 (4.18)	8.41 (8.30)
$[(C_{18}H_{17}N_3O_3S)_2Ni]$	74	>300	47	3.56	766.50	56.19 (56.34)	10.57 (10.96)	4.13 (4.20)	8.29 (8.36)
$[(C_{18}H_{17}N_3O_3S)_2Co]$	65	>300	63	4.81	765.74	56.24 (56.32)	10.69 (10.95)	4.10 (4.20)	8.17 (8.35)
$[(C_{18}H_{17}N_3O_3S)_2Cd]$	78	>300	68	–	823.22	52.73 (52.65)	10.30 (9.85)	3.66 (3.93)	7.55 (7.81)

FT-IR spectroscopy: FT-IR spectra of all the prepared Schiff base ligand and its metal(II) complexes clearly showed a difference with FT-IR peaks. The peak observed at 1652 cm^{-1} was due to the azomethine ν(C=N) stretching, which shifted to a lower wave value (1634-1622 cm^{-1}) in the complexes indicating the participation of azomethine nitrogen in coordination with the metal ion (N-M) [48]. The phenolic ν(O-M) stretching vibration band was observed at 1349 cm^{-1} in the free ligand. In metal(II) complexes, this band appeared at lower frequency 1036-1018 cm^{-1} region, confirming the participation of the phenolic group in complex formation [49]. The vibration bands for the SO_2 group in the free ligand molecule appeared at 1316 cm^{-1} and 1188 cm^{-1} $\nu_{asym}(SO_2)$ and $\nu_{asym}(SO_2)$, respectively. In the metal(II) complexes, the asym/symm. bands shifted to 1266-1222 and 1134-1112 cm^{-1}, respectively, upon the coordination of the central metal ion [49-54]. The additional peaks observed in metal complexes in the range of 460-419 cm^{-1} were due to N-M bonding and 517-509 cm^{-1} were due to O-M bonding [55,56]. The characteristic bands of the stretching frequency are listed in Table-2.

UV-Visible spectra and magnetic moment: UV-visible spectra of the synthesized Schiff base ligand and its metal(II) complexes were recorded in DMSO solvent (10^{-5} M). The absorption band in ligand molecule appeared at 320 nm and 274 nm for π→π* and n→π* transitions, respectively. These bands in metal(II) complexes were shifted at bathochromic shift. For Ni(II), Cd(II), Cu(II) and Co(II) complexes, the absorption bands appeared at 333 and 381, 343 and 389, 339 and 388, 352 and 390 nm, respectively. The absorption band at a bathochromic shift in metal complexes confirmed that the ligand moiety was coordinated with central metal ions [57].

The magnetic moment for Cu(II), Ni(II) and Co(II) complexes was calculated using the Gouy balance at 25 ºC. The observed magnetic moment values for Cu(II), Ni(II) and Cd(II) complexes were found to be 1.78, 3.56 and 4.81 B.M. respectively. The magnetic moment obtained for Cu(II) complex was approximately equal to spin-only value of one unpaired electron 1.75 B.M. for octahedral geometry [58]. In case of Ni(II) and Co(II) complexes, the observed magnetic moment values were approximately equal to its reported octahedral geometry [59-61].

ESR spectra: The X-band ESR spectra of copper(II) complex were recorded at liquid nitrogen temperature in DMSO solvent. Fig. 1 shown ESR spectra of Cu(II) complex. It provided information about the environment of the central metal ion in the complex. Covalency parameter α^2 was calculated to determine the bonding between central metal ions and surrounding ligand. The following equation was used to calculate the covalency parameter α^2:

$$\alpha^2 Cu(II) = - (A_{\parallel}0.036) + (g_{\parallel} - 2.002) + 3/7\ (g_{\perp} - 2.002) + 0.04 \quad (1)$$

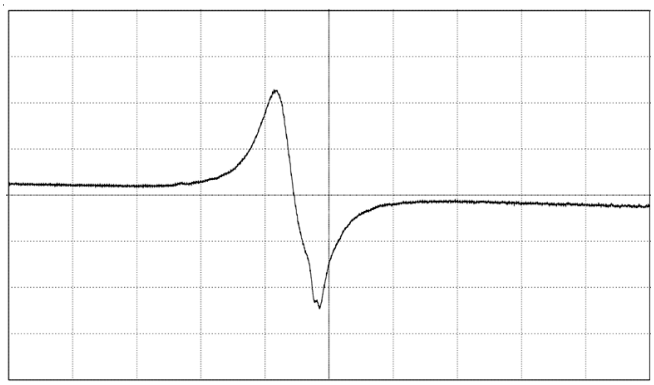

Fig. 1. ESR spectrum of Cu(II) complex

Hamilatoniaon parameter was used to calculate the ground state of the Cu(II) complex. All the calculated values are given in Table-3. The obtained $g_{\parallel}$ and $g_{\perp}$ values are greater than free electron g values. The trend in g values is $g_{\parallel} > g_{\perp} > 2.0023$, these values indicate that the unpaired electrons present in $d_{x^2-y^2}$ ground state, which are characteristics of octahedral geometry [62]. The calculated G value (axial symmetry parameter) was found to be > 4, which suggested that the interactions of Cu-Cu ions are negligible [63]. The effective magnetic moment was calculated using equation:

$$\mu_{eff}^2 = \frac{3}{4}\left(g_{av}^2\right)$$

TABLE-2
KEY FT-IR FREQUENCY (cm^{-1}) OF QUINOLINE SCHIFF BASE LIGAND AND ITS METAL(II) COMPLEXES

Compounds	ν(C=N)	ν(C-O)	ν(N-M)	ν(O-M)	$\nu_{asym}(SO_2)$	$\nu_{asym}(SO_2)$
$C_{18}H_{17}N_3O_3S$	1652	1349	–	–	1316	1188
$[(C_{18}H_{17}N_3O_3S)_2Cu]$	1622	1035	460	517	1246	1112
$[(C_{18}H_{17}N_3O_3S)_2Ni]$	1632	1036	419	510	1223	1125
$[(C_{18}H_{17}N_3O_3S)_2Co]$	1634	1018	459	516	1222	1134
$[(C_{18}H_{17}N_3O_3S)_2Cd]$	1633	1035	452	509	1266	1125

TABLE-3
ESR SPECTRAL DATA OF Cu(II) COMPLEX

$g_{\perp}$	$G_{\parallel}$	g_{av}	G	α^2	μ_{eff} (BM)
2.045	2.199	2.096	4.606	0.178	1.80

Thermogravimetric analysis: Table-4 summarized with decomposition stages, temperature range, loss of weight and assignments of the loss fragments. All the complexes start decomposed near 200 ºC, which indicates an absence of water moiety. The TG curve of the Co complex is shown in Fig. 2. The thermogram of Co^{2+} complex exhibited three decomposition stages. In stage first, the 12.19% weight loss (calculated 13.2%) was observed between the temperature range 200-240 ºC, corresponding to loss of C_8H_7 ligand moiety. In the second stage, 28.97% weight loss was observed (calcd. 28.10%) in the temperature range 280-680 ºC, due to loss of $C_{11}H_9N_3O_2$ moiety of the coordinated ligand molecule. In step third, 23.88% loss was observed (calculated 23.80%) in the range of 720-980 ºC with loss of $C_8H_9N_2O_5$ moiety. In the end, 21.91% residue remains present. The remaining residue contains metal oxide along with non-decomposed organic moiety.

Mass spectra: To confirm the complete formation, all the metal(II) complexes were subjected to ESI-MS. The ESI-MS spectrum of Ni(II) complex (Fig. 3) shows a molecular ion peak at $M^{\bullet+}$ 766, which corresponds to its molecular weight. Ligand, Cu(II), Co(II) and Cd(II) metal complexes show molecular ion peak at $M^{\bullet+}$ 356, 771, 765 and 823, respectively. The obtained molecular ion peaks of prepared compounds are exactly matched with its corresponding molecular weight. From

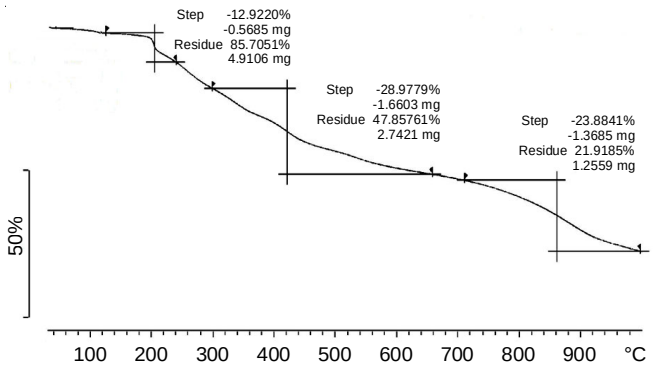

Fig. 2. TGA of Co(II) complex

study of ESI-MS spectra, it was confirmed that the synthesized compounds are completely formed.

Antibacterial activity: The prepared compounds have been screened for antibacterial activity with two Gram-positive and two Gram-negative bacterial strains. Among the prepared compounds, Schiff base ligand and its Cd(II) complex showed excellent activity with all four bacterial strains. In case of Cu(II), Co(II) and Ni(II) complexes, Cu(II) complex showed excellent activity against *E. coli* and *P. aeruginosa* bacterial strains (Fig. 4). Cobalt(II) complex has shown good to excellent activity again *E. coli*, *S. aureus* and *S. pyogenus* bacterial strain. Ni(II) complex was found to be weak active against the four bacterial strains.

Antifungal activity: All the synthesized compounds were screened against three fungal strain *viz.*, *C. albicans*, *A. niger* and *A. clavatus* at different concentrations ranging between

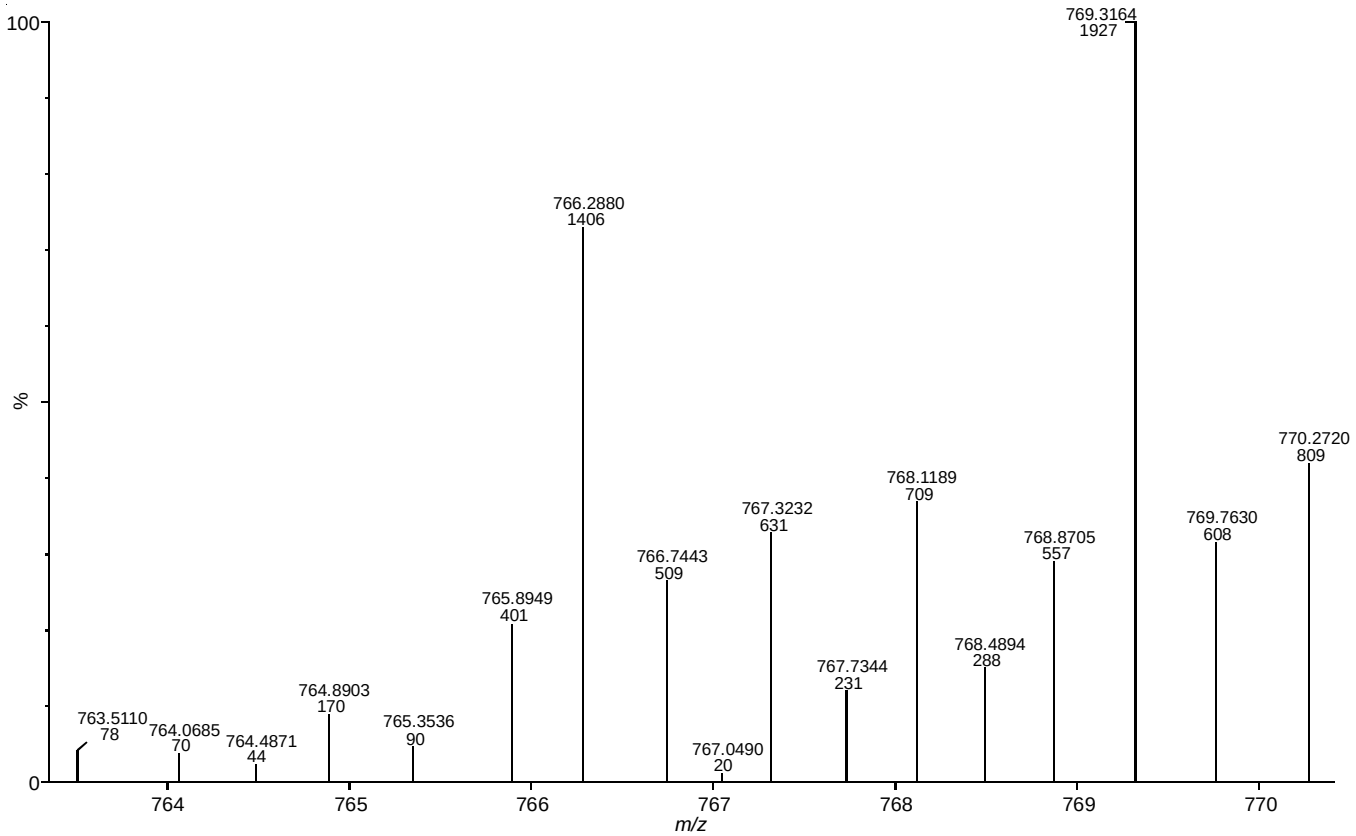

Fig. 3. ESI-MS of Ni complex

TABLE-4
STEPWISE THERMAL DECOMPOSITION STUDY OF QUINOLINE SCHIFF BASE METAL(II) COMPLEXES

Complex	Decomposition temp. (°C)	Weight loss (%)		Interference
		Observed	Calculated	
$[(C_{18}H_{17}N_3O_3S)_2Co]$	200-240	12.92	13.22	C_8H_7
	280-680	28.97	28.10	$C_{11}H_9N_3O_2$
	720-980	23.88	23.80	$C_8H_9N_2O_5$
	Residue	21.91	33.90	$CoO + C_9H_7NO_2S$
$[(C_{18}H_{17}N_3O_3S)_2Cu]$	200-460	44.38	44.10	$C_{18}H_{16}N_3O_2S$
	550-980	16.56	16.80	C_9H_7N
	Residue	33.16	32.90	$CuO + C_9H_9N_2O_3S$
$[(C_{18}H_{17}N_3O_3S)_2Ni]$	220-340	16.15	16.90	C_9H_7N
	350-640	21.65	22.15	$C_7H_8NO_2S$
	660-980	18.15	18.10	C_7H_7OS
	Residue	36.83	40.90	$NiO + C_{13}H_{10}N_4O_2$
$[(C_{18}H_{17}N_3O_3S)_2Cd]$	180-260	13.84	14.21	C_8H_7N
	280-540	25.03	25.30	$C_9H_9N_2O_2S$
	560-980	22.53	22.43	$C_7H_8N_2O_2S$
	Residue	31.19	37.90	$CdO + C_{12}H_8NO$

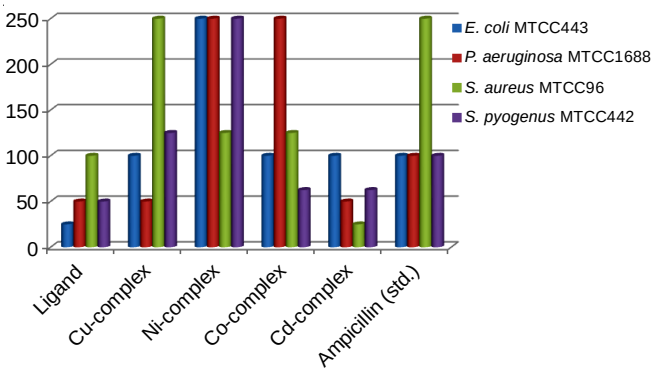

Fig. 4. Antibacterial activity of ligand and its metal complexes (MIC, mg mL^{-1})

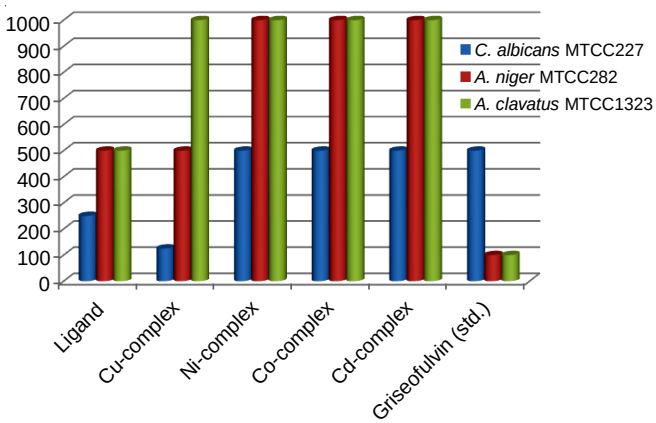

Fig. 5. Antifungal activity of ligand and its metal complexes (MIC, mg mL^{-1})

100 and 1250 µg/mL using agar plate method. Among the synthesized compounds ligand molecule has shown good activity with all three fungal strains. In metal(II) complexes, Cu(II) complex showed excellent activity against fungal strain *C. albicans*. Co(II), Ni(II) and Cd(II) complexes exhibit good activity against fungal strain *C. albicans* (Fig. 5).

Cytotoxicity: The *in vitro* cytotoxicity of ligand and its metal(II) complexes was investigated against A-549 (human lung cancer) and MCF-7 (human breast cancer) cell lines and results are tabulated in Table-5. Paclitaxel was used as the standard drug during the activity. The ligand and its metal(II) complexes showed inhibition of cell value IC_{50} in the range 33.55-47.61 µM for A-549 and 30.95-46.81 µM for MCF-7 cell lines. The ligand and its metal complexes exhibited higher activity against the A-549 cancer cell line and lowered in the case of the MCF-7 cancer cell line compared to standard. The obtained results showed that the most of the synthesized metal complexes were found to be more active than their corresponding ligand molecule (Fig. 6). The order of activity of all the synthesized compounds against the A-549 cancer cell line is

TABLE-5
HYDROGEN BONDING INTERACTIONS OF β-TUBULIN WITH
VARIOUS QUINOLINE SCHIFF BASE LIGAND METAL(II) COMPLEXES

Complexes	Binding energy (kcal/mol)	Atoms involved in the bonding interactions	Distance atom pair	Angle	Figure
Cd-Metal	-11.32	Drg-1:H – O-THR276 ARG278:N - HC-Drg	1.76776 3.5812	143.055	8A
Co-Metal	-10.70	Drg-H - O-THR276 ARG278-N – HC-UNL	1.78816 3.58511	149.203	8B
Cu-Metal	-12.39	Drg:H - O-THR276 Drg:CH - O-THR276 Drg:CH - O-ALA233 ARG278-N – HC-Drg	1.95704 2.91936 3.63567 3.83767	123.983	8C
Ni-Metal	-11.39	Drg-CH - O-THR276 ASP226:O – HC-Drg	1.7098 3.15848	157.537	8D

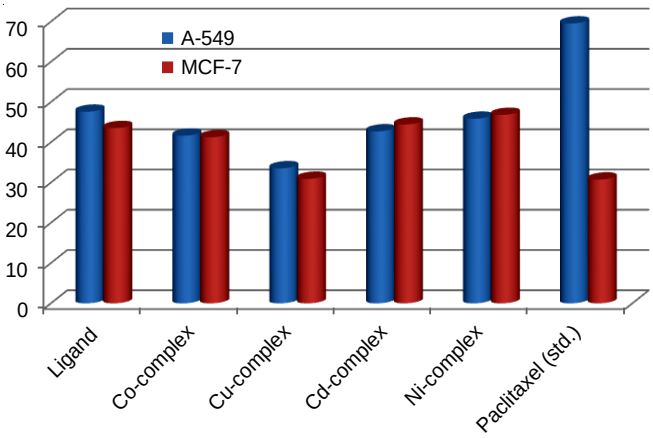

Fig. 6. *In vitro* cytotoxicity of ligand and metal complexes

Cu > Co > Cd > Ni-complex > ligand and for MCF-7 cancer cell line Cu > Co > Cd > ligand > Ni-complex.

Molecular docking of β-tubulin with drug-metal complexes: We employed molecular docking, to investigate the interaction of metal complexes (Cd, Co, Cu and Ni) with β-tubulin through AutoDock4.2 [43]. The lowest binding energy conformation of metal complexes (Cd, Co, Cu and Ni) with β-tubulin was found at -11.32, -10.70, -12.39 and -11.39 kcal/mol, respectively. All the metal(II) complexes show a considerable binding energy and affinity with β-tubulin as shown in Fig. 7. The analysis of β-tubulin-Cd metal complex show the conventional hydrogen bonding interaction of residue Thr276 (1.76 Å) and carbon hydrogen bonding interaction with Arg278 (3.58 Å) (Table-5). The Asp226 show electrostatic interactions, Thr220, Thr223, Phe272, Ser277, Gln282, Arg284 forms van der Waals interactions, Arg273 forms π-lone pair and Asp226 makes π-anion type of interactions with Cd-metal complex as shown in Fig. 8A. While, Leu217, Lys218, Leu219, His229, Pro274, Leu371, Leu285, Pro360 forms hydrophobic interactions with drug-Cd complex as shown in Fig. 8A. Next, analysis of β-tubulin-Cd metal complex is stabilized by hydrogen bonding interaction of Thr276 (1.78 Å) and carbon hydrogen bonding interaction with Arg278 (3.58 Å) shown in (Fig. 8B), similar to β-tubulin-Cd metal complex (Fig. 8A). Also, β-tubulin-Co metal complex shows non bonded interaction such as Thr220, Thr223, Ser277, Gln282 forms van der Waals, Asp226 forms π- anion, His-229 makes π-π T-shaped interaction and Leu217, Lys218, Leu219, Pro274, Leu286, Leu371 and Pro360 forms hydrophobic alkyl and π-alkyl types of interactions with drug-Cd as shown in Fig. 8B.

The analysis of β-tubulin-Cu metal complex shows the hydrogen bonding interactions of Thr276 (1.95 and 2.91 Å) (Table-5) and carbon bonding interactions Ala233 (3.63 Å) and Arg278 (3.83 Å) shown in (Fig. 8C). In addition, Arg278 makes π-donon bonding interaction, Leu371 makes π-sigma bonding, Asp226 forms π-anion, His229 forms π-π T-shaped interactions with drug-Cu metal complex and Leu217, Leu219 and Pro274 forms hydrophobic alkyl and π-alkyl type of interactions as shown in Fig. 8C. Next, analysis of β-tubulin-Ni metal complex show bonding interactions with Thr276 (1.70 Å) and carbon bonding interactions Asp226 (3.15 Å) as shown in Fig. 8D. Leu217, Thr220, Thr223, His229, Arg284, Gln282, Gly370 and Leu371 forms van der Waals interactions, Asp226 forms π-anion, Lys281 forms amide-π stacked as shown in Fig. 8D. While, Leu219, Arg278, Pro360 forms hydrophobic type of alkyl and π-alkyl type of interactions as shown Fig. 8D.

Conclusion

A novel quinoline Schiff base ligand and its metal(II) complexes were successfully prepared and characterized. The synthesized Schiff base and its metal(II) complexes were screened for antibacterial, antifungal and cytotoxicity activities. Among the prepared compounds, the Schiff base ligand and its Cd(II) complex showed an excellent activity against all four

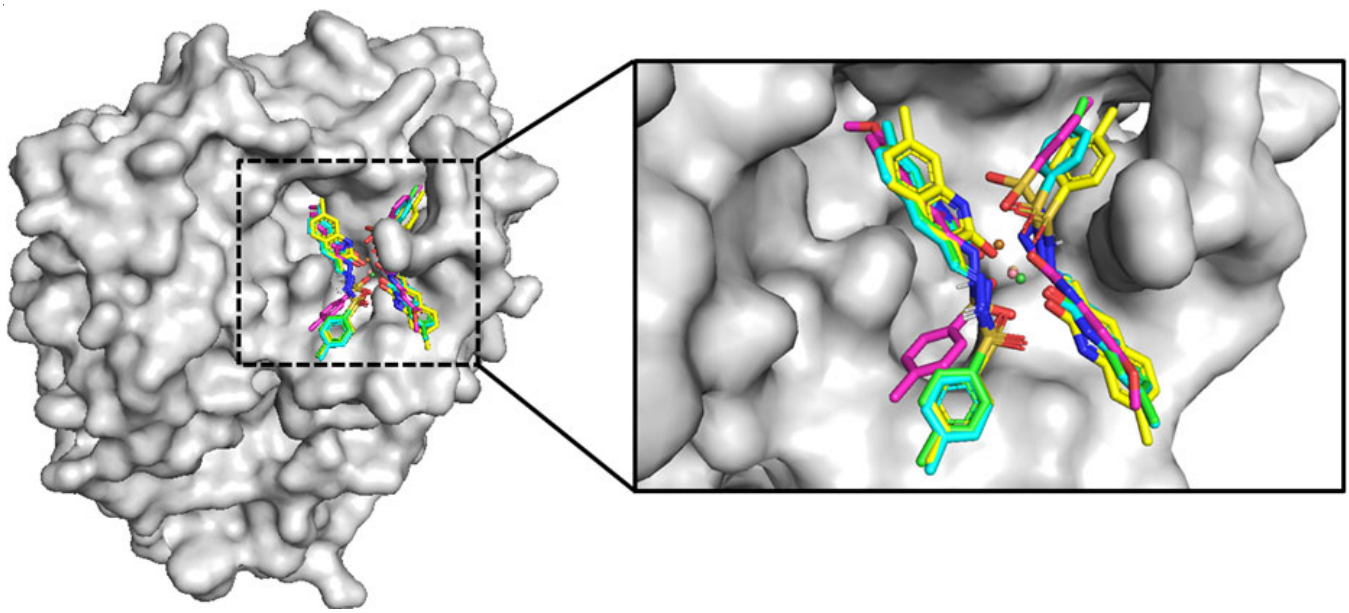

Fig. 7. Molecular docking of β-tubulin with drug-metal complexes. Here, (A) shows the overlapped docked conformation of Cd (green), Co (cyan), Cu (magenta) and Ni (yellow) metal complexes, the atoms such as N, O and H are shown in blue, red and white colour, respectively. (B) Zoomed view of β-tubulin binding pocket with overlapped conformation of metal complexes

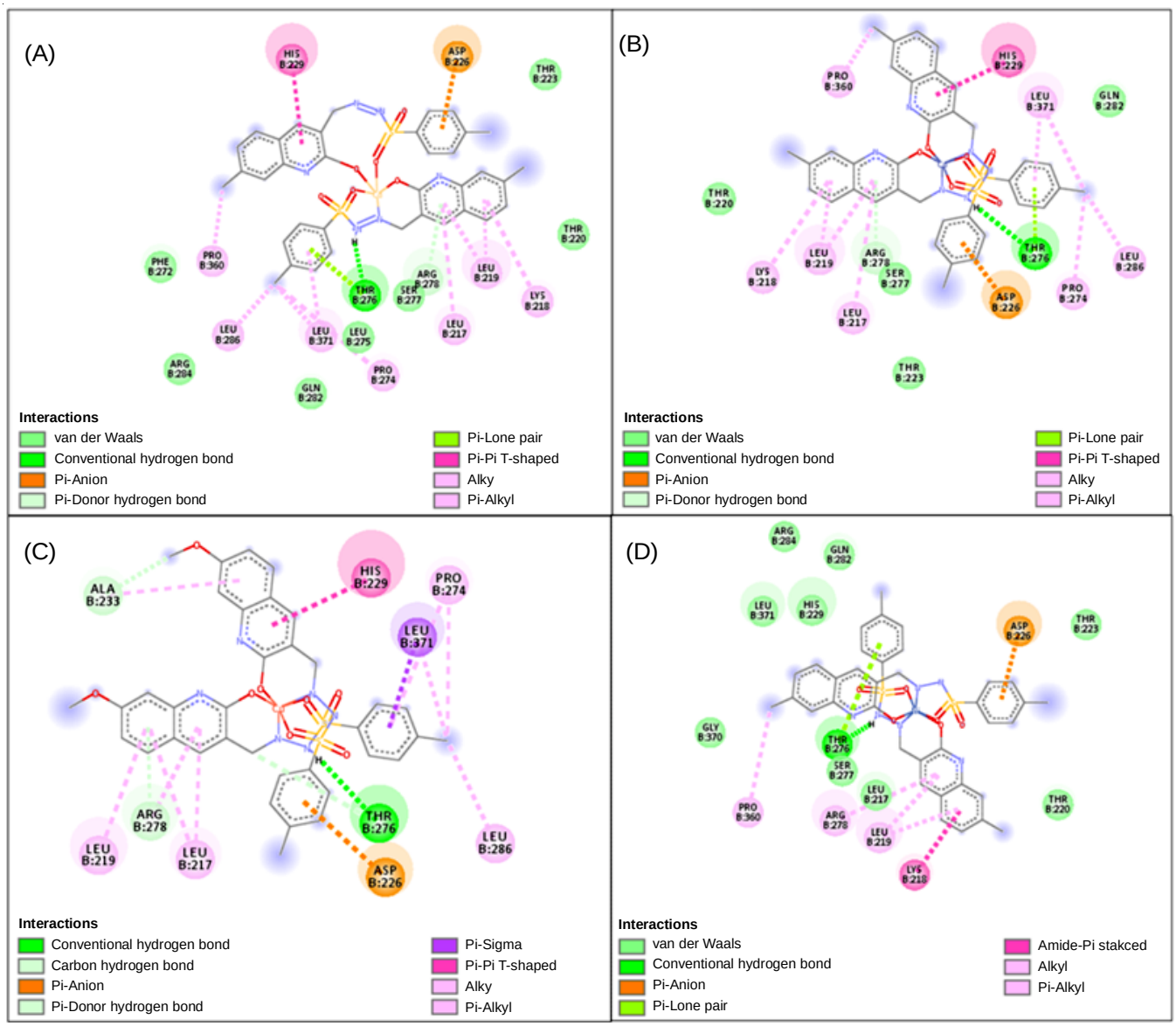

Fig. 8. Interaction networks of β-tubulin residues with drug metal complexes. (A) Interaction network of β-tubulin residues with Cd-metal complex (B.E. = -11.32 kcal/mol), (B) Interaction network of β-tubulin residues with Co-metal complex (B.E. = -10.70 kcal/mol), (C) shows interaction of β-tubulin with Cu-metal complex (B.E. = -12.39 kcal/mol) and (D) Interaction network of β-tublin with Ni-metal complex (B.E. = -11.39 kcal/mol). The β-tubulin shows higher binding affinity for Cu-metal complex compare to other tubulin and metal complexes, this result is in agreement with the experimental observation. The 2D interaction images were generated using the Discovery studio Visualizer [46]

bacterial strains. In case of antifungal activity ligand and Cu(II) complex exhibited good activity against *A. clavatus* fungal strain. Other compounds were found to be less active against both bacterial and fungal strains. Furthermore, all the compounds were screened for *in vitro* cytotoxicity against two human cancer cell lines and results showed that the Cu(II) complex was found to be more active among the prepared compounds. The Schiff base ligand, Co(II), Ni(II) and Cd(II) compounds showed excellent activity against the human lung cancer cell line (A-549). From overall study, it was concluded that all compounds have excellent cytotoxicity properties compared to the standard drug paclitaxel. Ligand and Cd(II) complex has excellent antibacterial activity compared to the standard drug Ampicillin. Furthermore, the binding modes and interactions of metal complexes with β-tubulin receptor protein are confirmed by molecular docking study. The docking study revealed that all the metal(II) complexes show excellent binding affinity at the paclitaxel site of the β-tubulin. Hence, it is concluded that prepared compounds possessed excellent cytotoxicity properties and could be used as potential lead for cancer treatment.

ACKNOWLEDGEMENTS

The authors would like to extend their sincere appreciation to the Department of Chemistry, C.K.T. College, New Panvel, India for providing the laboratory and research facilities.

CONFLICT OF INTEREST

The authors declare that there is no conflict of interests regarding the publication of this article.

REFERENCES

1. S.A. Sadeek, M.S. El-Attar and S.M. Abd El-Hamid, *J. Mol. Struct.*, **1051**, 30 (2013); https://doi.org/10.1016/j.molstruc.2013.07.053
2. B. Vivekanand, K. Mahendra Raj and B.H.M. Mruthyunjayaswamy, *J. Mol. Struct.*, **1079**, 214 (2015); https://doi.org/10.1016/j.molstruc.2014.08.033
3. E. Labisbal, J.A. Garcia-Vazquez, J. Romero, S. Picos, A. Sousa, A. Castiñeiras and C. Maichle-Mössmer, *Polyhedron*, **14**, 663 (1995); https://doi.org/10.1016/0277-5387(94)00292-M
4. S.A. Beyramabadi, B. Esmaeili, A. Gharib, M. Khorsandi-Chenarboo, A. Morsali, M. Khashi and R. Sanavi-Khoshnood, *J. Mol. Struct.*, **1146**, 620 (2017); https://doi.org/10.1016/j.molstruc.2017.06.050
5. A. Beyramabadi, A. Morsali, M.J. Khoshkholgh and A.A. Esmaeili, *Spectrochim. Acta A Mol. Biomol. Spectrosc.*, **83**, 467 (2011); https://doi.org/10.1016/j.saa.2011.08.067
6. M. Habibi, S.A. Beyramabadi, S. Allameh, M. Khashi, A. Morsali, M. Pordel and M. Khorsandi-Chenarboo, *J. Mol. Struct.*, **1143**, 424 (2017); https://doi.org/10.1016/j.molstruc.2017.04.114
7. T. Toozandejani, S.A. Beyramabadi, H. Chegini, M. Khashi, A. Morsali and M. Pordel, *J. Mol. Struct.*, **1127**, 15 (2017); https://doi.org/10.1016/j.molstruc.2016.07.026
8. M. Yavari, S.A. Beyramabadi, A. Morsali and M.R. Bozorgmehr, *J. Struct. Chem.*, **59**, 1102 (2018); https://doi.org/10.1134/S0022476618050128
9. A.A. Abdel Aziz, F.M. Elantabli, H. Moustafa and S.M. El-Medani, *J. Mol. Struct.*, **1141**, 563 (2017); https://doi.org/10.1016/j.molstruc.2017.03.081
10. E.G. Bakirdere, M.F. Fellah, E. Canpolat, M. Kaya and S. Gür, *J. Serb. Chem. Soc.*, **81**, 509 (2016); https://doi.org/10.2298/JSC151030008B
11. S. Dutta Gupta, B. Revathi, G.I. Mazaira, M.D. Galigniana, C.V.S. Subrahmanyam, N.L. Gowrishankar and N.M. Raghavendra, *Bioorg. Chem.*, **59**, 97 (2015); https://doi.org/10.1016/j.bioorg.2015.02.003
12. S.A. Elsayed, A.M. Noufal and A.M. El-Hendawy, *J. Mol. Struct.*, **1144**, 120 (2017); https://doi.org/10.1016/j.molstruc.2017.05.020
13. S.H. Sumrra, S. Kausar, M.A. Raza, M. Zubair, M.N. Zafar, M.A. Nadeem, E.U. Mughal, Z.H. Chohan, F. Mushtaq and U. Rashid, *J. Mol. Struct.*, **1168**, 202 (2018); https://doi.org/10.1016/j.molstruc.2018.05.036
14. P. Tyagi, S. Chandra, B.S. Saraswat and D. Yadav, *Spectrochim. Acta A Mol. Biomol. Spectrosc.*, **145**, 155 (2015); https://doi.org/10.1016/j.saa.2015.03.034
15. C. Chandramouli, M. Shivanand, T. Nayanbhai, B. Bheemachari and R. Udupi, *J. Chem. Pharm. Res.*, **4**, 1151 (2012).
16. B.S. Creaven, M. Devereux, D. Karcz, A. Kellett, M. McCann, A. Noble and M. Walsh, *J. Inorg. Biochem.*, **103**, 1196 (2009); https://doi.org/10.1016/j.jinorgbio.2009.05.017
17. A.R. Gholap, K.S. Toti, F. Shirazi, R. Kumari, M.K. Bhat, M.V. Deshpande and K.V. Srinivasan, *Bioorg. Med. Chem.*, **15**, 6705 (2007); https://doi.org/10.1016/j.bmc.2007.08.009
18. R. Joshi, A. Kumari, K. Singh, H. Mishra and S. Pokharia, *J. Mol. Struct.*, **1197**, 519 (2019); https://doi.org/10.1016/j.molstruc.2019.07.066
19. H. Vural and Ö. Idil, *J. Mol. Struct.*, **1177**, 242 (2019); https://doi.org/10.1016/j.molstruc.2018.09.070
20. E. Khan, M. Hanif and M.S. Akhtar, *Rev. Inorg. Chem.*, (2021); https://doi.org/10.1515/revic-2021-0034
21. F. Ghasedian, H. Zamani, F. Joz-Yarmohammadi, S. Beyramabadi and M. Abedi, *Russ. J. Appl. Chem.*, **89**, 2001 (2016); https://doi.org/10.1134/S1070427216120119
22. S. Calus, E. Gondek, A. Danel, B. Jarosz, M. Pokladko and A. Kityk, *Mater. Lett.*, **61**, 3292 (2007); https://doi.org/10.1016/j.matlet.2006.11.055
23. A. Soroceanu, M. Cazacu, S. Shova, C. Turta, J. Ko•íšek, M. Gall, M. Breza, P. Rapta, T.C.O. Mac Leod, A.J.L. Pombeiro, J. Telser, A.A. Dobrov and V.B. Arion, *Eur. J. Inorg. Chem.*, **2013**, 1458 (2013); https://doi.org/10.1002/ejic.201201080
24. F. Jafari-Moghaddam, S.A. Beyramabadi, M. Khashi and A. Morsali, *J. Mol. Struct.*, **1153**, 149 (2018); https://doi.org/10.1016/j.molstruc.2017.10.007
25. C.C. Roberts, B.R. Barnett, D.B. Green and J.M. Fritsch, *Organometallics*, **31**, 4133 (2012); https://doi.org/10.1021/om200865w
26. Z.A. Siddiqi, M. Khalid, S. Kumar, M. Shahid and S. Noor, *Eur. J. Med. Chem.*, **45**, 264 (2010); https://doi.org/10.1016/j.ejmech.2009.10.005
27. Z.-C. Liu, B.-D. Wang, B. Li, Q. Wang, Z.-Y. Yang, T.-R. Li and Y. Li, *Eur. J. Med. Chem.*, **45**, 5353 (2010); https://doi.org/10.1016/j.ejmech.2010.08.060
28. P. Hewawasam, W. Fan, J. Knipe, S.L. Moon, C.G. Boissard, V.K. Gribkoff and J.E. Starrett Jr., *Bioorg. Med. Chem. Lett.*, **12**, 1779 (2002); https://doi.org/10.1016/S0960-894X(02)00240-8
29. M.A. Abd-Alla, A.-H.N. Ahmed, M.F. El-Zohry and F.A. Omar, *Collect. Czech. Chem. Commun.*, **57**, 1547 (1992); https://doi.org/10.1135/cccc19921547
30. B.S. Holla, M. Mahalinga, M.S. Karthikeyan, P.M. Akberali and N.S. Shetty, *Bioorg. Med. Chem.*, **14**, 2040 (2006); https://doi.org/10.1016/j.bmc.2005.10.053
31. M. Andaloussi, E. Moreau, N. Masurier, J. Lacroix, R.C. Gaudreault, J.-M. Chezal, A. El Laghdach, D. Canitrot, E. Debiton, J.-C. Teulade and O. Chavignon, *Eur. J. Med. Chem.*, **43**, 2505 (2008); https://doi.org/10.1016/j.ejmech.2008.02.017
32. P. Rani, V. Srivastava and A. Kumar, *Eur. J. Med. Chem.*, **39**, 449 (2004); https://doi.org/10.1016/j.ejmech.2003.11.002
33. N. Hamdi, C. Lidrissi, M. Saoud, A. Romerosa Nievas and H. Zarrouk, *Chem. Heterocycl. Compd.*, **42**, 320 (2006); https://doi.org/10.1007/s10593-006-0088-0
34. G. Paolucci, A. Zanella, L. Sperni, V. Bertolasi, M. Mazzeo and C. Pellecchia, *J. Mol. Catal. Chem.*, **258**, 275 (2006); https://doi.org/10.1016/j.molcata.2006.05.043
35. J.-Q. Wu, L. Pan, Y.-G. Li, S.-R. Liu and Y.-S. Li, *Organometallics*, **28**, 1817 (2009); https://doi.org/10.1021/om801028g
36. X. Wang, R. Fan, Y. Dong, T. Su, J. Huang, X. Du, P. Wang and Y. Yang, *Cryst. Growth Des.*, **17**, 5406 (2017); https://doi.org/10.1021/acs.cgd.7b00891
37. B.M. Mistry, S.K. Sahoo and S. Jauhari, *J. Electroanal. Chem.*, **704**, 118 (2013); https://doi.org/10.1016/j.jelechem.2013.07.004
38. S.K. Patil and B.T. Vibhute, *Arab. J. Chem.*, **14**, 103285 (2021); https://doi.org/10.1016/j.arabjc.2021.103285
39. S. Adsule, V. Barve, D. Chen, F. Ahmed, Q.P. Dou, S. Padhye and F.H. Sarkar, *J. Med. Chem.*, **49**, 7242 (2006); https://doi.org/10.1021/jm0607121
40. A. Srivastava and R.M. Singh, *Indian J. Chem.*, **44A**, 1868 (2005).
41. I. Wiegand, K. Hilpert and R.E.W. Hancock, *Nat. Protoc.*, **3**, 163 (2008); https://doi.org/10.1038/nprot.2007.521
42. H.R. Rajabi, R. Naghiha, M. Kheirizadeh, H. Sadatfaraji, A. Mirzaei and Z.M. Alvand, *Mater. Sci. Eng. C*, **78**, 1109 (2017); https://doi.org/10.1016/j.msec.2017.03.090
43. G.M. Morris, R. Huey, W. Lindstrom, M.F. Sanner, R.K. Belew, D.S. Goodsell and A.J. Olson, *J. Comput. Chem.*, **30**, 2785 (2009); https://doi.org/10.1002/jcc.21256
44. R.H. Wade and A.A. Hyman, *Curr. Opin. Cell Biol.*, **9**, 12 (1997); https://doi.org/10.1016/S0955-0674(97)80146-9
45. R.A. Stanton, K.M. Gernert, J.H. Nettles and R. Aneja, *Med. Res. Rev.*, **31**, 443 (2011); https://doi.org/10.1002/med.20242
46. BIOVIA DS, Discovery Studio Modeling Environment, Release 2017, San Diego. In: Dassault Systèmes (2016).

47. W.L. DeLano, The PyMOL Molecular Graphics System, Version 1.1. Schrödinger LLC (2002).
48. M. Pervaiz, I. Ahmad, M. Yousaf, S. Kirn, A. Munawar, Z. Saeed, A. Adnan, T. Gulzar, T. Kamal, A. Ahmad and A. Rashid, *Spectrochim. Acta A Mol. Biomol. Spectrosc.*, **206**, 642 (2019); https://doi.org/10.1016/j.saa.2018.05.057
49. N. Raman, A. Kulandaisamy and K. Jeyasubramanian, *Synth. React. Inorg. Met.-Org. Chem.*, **31**, 1249 (2001); https://doi.org/10.1081/SIM-100106862
50. N. Sari, S. Arslan, E. Logoglu and I. Sakiyan, *J. Am. Sci.*, **16**, 283 (2003).
51. G. Mohamed and Z. Abd El-Wahab, *J. Therm. Anal. Calorim.*, **73**, 347 (2003); https://doi.org/10.1023/A:1025126801265
52. A.S. Salameh and H.A. Tayim, *Polyhedron*, **2**, 829 (1983); https://doi.org/10.1016/S0277-5387(00)87213-7
53. H.S. Seleem, B.A. El-Shetary and M. Shebl, *Heteroatom Chem.*, **18**, 100 (2007); https://doi.org/10.1002/hc.20239
54. M. Shebl and S.M.E. Khalil, *Monatsh. Chem.*, **146**, 15 (2015); https://doi.org/10.1007/s00706-014-1302-x
55. M. Shebl, *J. Coord. Chem.*, **62**, 3217 (2009); https://doi.org/10.1080/00958970903012785
56. M. Shebl, *J. Mol. Struct.*, **1128**, 79 (2017); https://doi.org/10.1016/j.molstruc.2016.08.056
57. P. Tyagi, S. Chandra and B.S. Saraswat, *Spectrochim. Acta A Mol. Biomol. Spectrosc.*, **134**, 200 (2015); https://doi.org/10.1016/j.saa.2014.06.112
58. D.P. Singh, R. Kumar, V. Malik and P. Tyagi, *Transition Met. Chem.*, **32**, 1051 (2007); https://doi.org/10.1007/s11243-007-0279-2
59. N.N. Greenwood and A. Earnshaw, Chemistry of the Elements, Heimemann: Oxford, UK, Ed.: 2 (1997).
60. T.R. Rao and A. Prasad, *Met.-Org. Nano-Met. Chem.*, **35**, 299 (2005); https://doi.org/10.1081/SIM-200055245
61. B.T. Thaker, P.K. Tandel, A.S. Patel, C.J. Vyas, M.S. Jesani and D.M. Patel, *Indian J. Chem.*, **44A**, 265 (2005)
62. G. Reddy, S. Balasubramanian and K. Chennakesavulu, *J. Mater. Chem. A Mater. Energy Sustain.*, **2**, 19102 (2014); https://doi.org/10.1039/C4TA90172J
63. H.F. El-Shafiy and M. Shebl, *J. Mol. Struct.*, **1156**, 403 (2018); https://doi.org/10.1016/j.molstruc.2017.11.081